21

Earthquake Dynamics of Base-Isolated Buildings

PREVIEW

The concept of protecting a building from the damaging effects of an earthquake by introducing some type of support that isolates it from the shaking ground is an attractive one, and many mechanisms to achieve this result have been proposed. Although the early proposals go back 100 years, it is only in recent years that *base isolation* has become a practical strategy for earthquake-resistant design. In this chapter we study the dynamic behavior of buildings supported on base isolation systems with the limited objective of understanding why and under what conditions isolation is effective in reducing the earthquake-induced forces in a structure. Base isolation is currently an active and expanding subject, however, and a large body of literature exists on various aspects of base isolation: testing and mechanics of hardware in isolation systems, nonlinear dynamic analysis, shaking table tests, design projects, field installation, and field performance.

21.1 ISOLATION SYSTEMS

Despite wide variation in detail, base isolation techniques follow two basic approaches with certain common features. In the first approach the isolation system introduces a layer of low lateral stiffness between the structure and the foundation. With this isolation layer the structure has a natural period that is much longer than its fixed-base natural period. As shown by the elastic design spectrum of Fig. 21.1.1, this lengthening of period can reduce the pseudo-acceleration and hence the earthquake-induced forces in the structure,

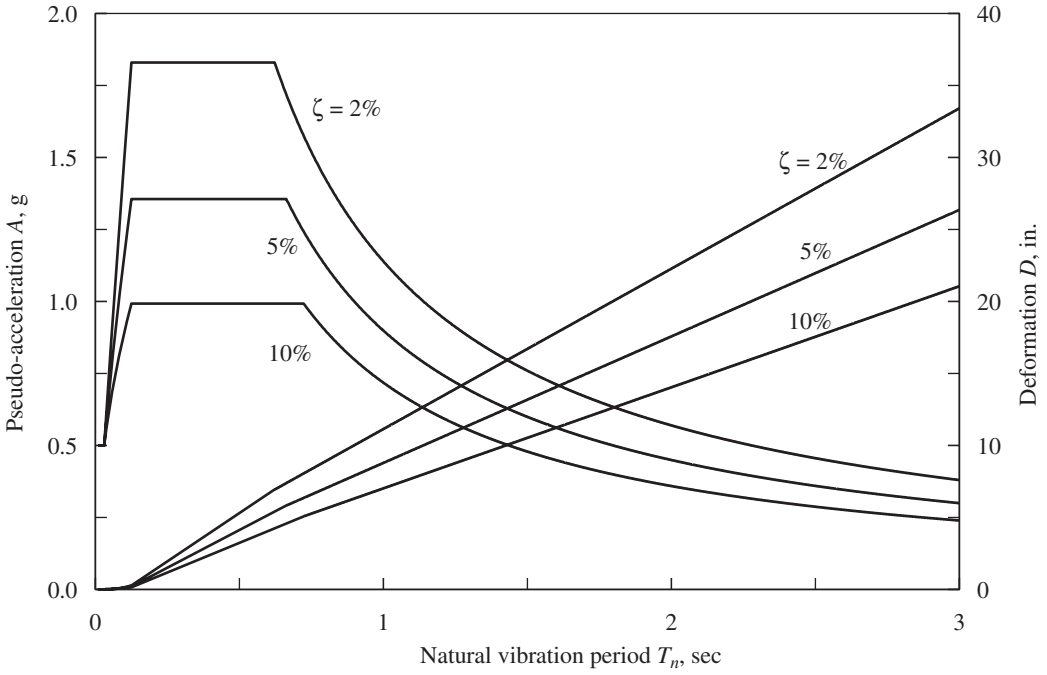

Figure 21.1.1 Elastic design spectrum.

but the deformation is increased; this deformation is concentrated in the isolation system, however, accompanied by only small deformations in the structure. This type of isolation system is effective even if the system is linear and undamped. Damping is beneficial, however, in further reducing the forces in the structure and the deformation in the isolation system.

The most common system of this type uses short, cylindrical bearings with one or more holes and alternating layers of steel plates and hard rubber (Fig. 21.1.2). Interposed between the base of the structure and the foundation, these laminated bearings are strong and stiff under vertical loads, yet very flexible under lateral forces (Fig. 21.1.3). Because the natural damping of the rubber is low, additional damping is usually provided by some form of mechanical damper. These have included lead plugs inserted into the holes, hydraulic dampers, steel bars, or steel coils. Metallic dampers provide energy dissipation through yielding, thus introducing nonlinearity in the system.

The second most common type of isolation system uses sliding elements between the foundation and the base of the structure. The shear force transmitted to the structure across the isolation interface is limited by keeping the coefficient of friction as low as practical. However, the friction must be sufficiently high to sustain strong winds and small earthquakes without sliding, a requirement that reduces the isolation effect. In this type of isolation system, the sliding displacements are controlled by high-tension springs or laminated rubber bearings, or by making the sliding surface curved; these

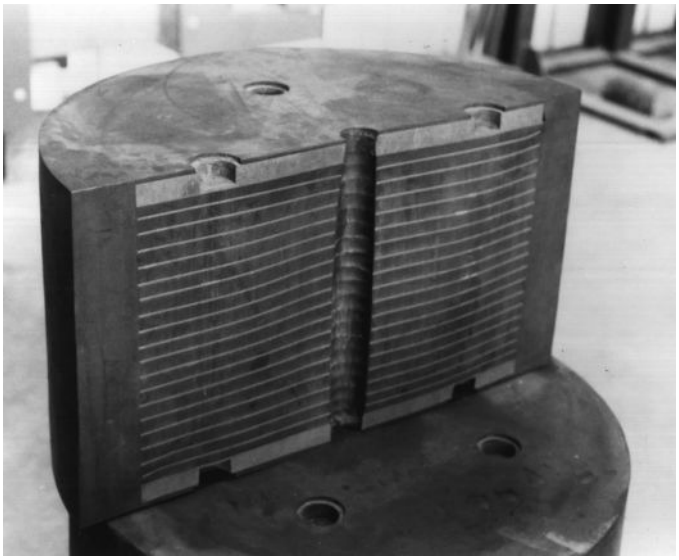

Figure 21.1.2 Section of a laminated rubber bearing. (Courtesy of I. D. Aiken.)

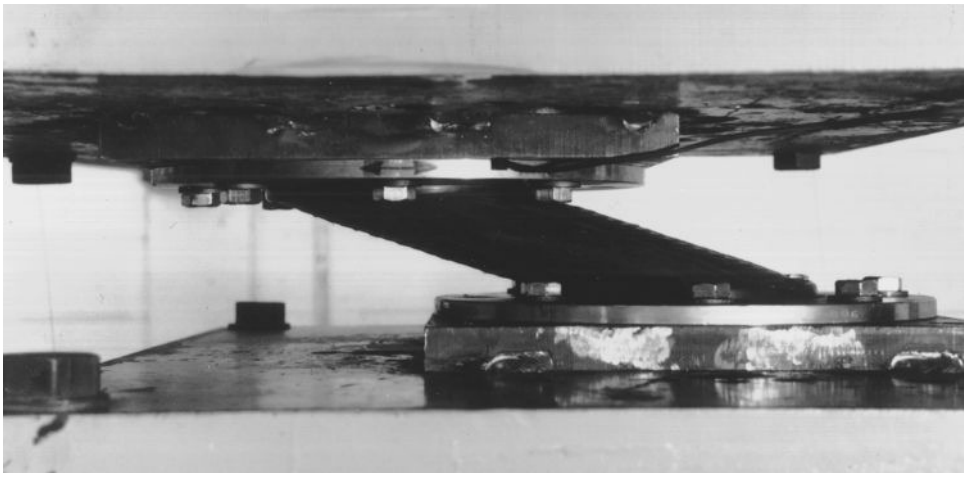

Figure 21.1.3 Deformed laminated rubber bearing. (Courtesy of I. D. Aiken.)

mechanisms provide a restoring force, otherwise unavailable in this type of system, to return the structure to its equilibrium position. The friction pendulum system (FPS) is a sliding isolation system wherein the weight of the structure is supported on spherical sliding surfaces that slide relative to each other when the ground motion exceeds a threshold level (Fig. 21.1.4). The restoring action is caused by raising the building slightly when sliding occurs on the spherical surface. The dynamics of structures on

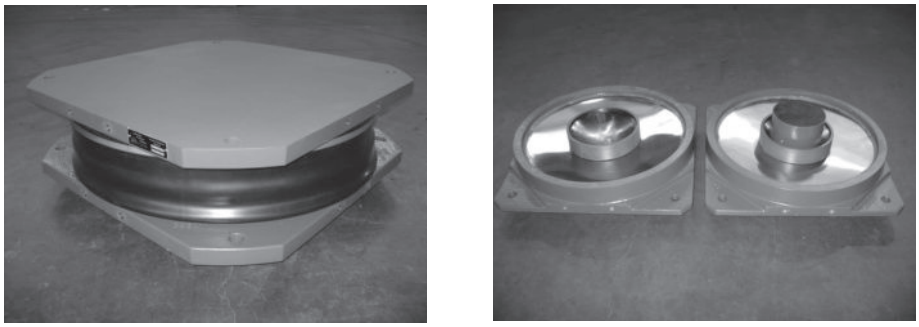

(a) (b)

Figure 21.1.4 (a) Friction pendulum sliding bearing; (b) internal components. (Courtesy of Earthquake Protection Systems.)

slider type of isolation systems is complicated because the slip process is intrinsically nonlinear.

To avoid this complication, this introductory presentation is limited to understanding the dynamic behavior of structures using the isolation system with laminated rubber bearings. Such isolated buildings are amenable to approximate analysis by the familiar modal analysis procedure (Chapter 13).

21.2 BASE-ISOLATED ONE-STORY BUILDINGS

In this section we identify why base isolation is effective in reducing the earthquake-induced forces in buildings. For this purpose we consider a one-story building with an isolation system between the base of the building and the ground. Most isolation systems are nonlinear in their force–deformation relationships, but it is not necessary to consider these nonlinear effects in this introductory treatment of the subject. A linear analysis of the system would serve our purpose of gaining insight into the dynamics of base-isolated buildings. Nonlinearity in the force–deformation relation should be considered for final design, however.

21.2.1 System Considered and Parameters

The one-story building to be isolated is shown idealized in Fig. 21.2.1a together with its properties: lumped mass m, lateral stiffness k, and damping coefficient c. This is the familiar SDF system with natural frequency ω_n, natural period T_n, and damping ratio ζ. Here we use the subscript f instead of n to emphasize that these are properties of the structure on a fixed base (i.e., without any isolation system); thus

$$\omega_f = \sqrt{\frac{k}{m}} \qquad T_f = \frac{2\pi}{\omega_f} \qquad \zeta_f = \frac{c}{2m\omega_f} \tag{21.2.1}$$

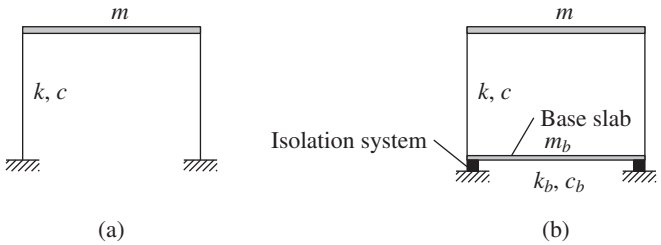

Figure 21.2.1 (a) Fixed-base structure; (b) isolated structure.

As shown in Fig. 21.2.1b, this one-story building is mounted on a base slab of mass m_b that in turn is supported on a base isolation system with lateral stiffness k_b and linear viscous damping c_b. Two parameters, T_b and ζ_b, are introduced to characterize the isolation system:

$$T_b = \frac{2\pi}{\omega_b} \qquad \text{where} \qquad \omega_b = \sqrt{\frac{k_b}{m + m_b}} \tag{21.2.2a}$$

$$\zeta_b = \frac{c_b}{2(m + m_b)\omega_b} \tag{21.2.2b}$$

We may interpret T_b as the natural vibration period, and ζ_b as the damping ratio, of the isolation system (with the building assumed to be rigid). For base isolation to be effective in reducing the forces in the building, T_b must be much longer than T_f, as we shall see later. The one-story building on a base isolation system (Fig. 21.2.1b) is a two-DOF system with mass, stiffness, and damping matrices denoted by $\mathbf{m}$, $\mathbf{k}$, and $\mathbf{c}$, respectively. The disparity between the high damping in rubber bearings and the low damping of the building means that damping in the combined system is nonclassical.

21.2.2 Analysis Procedure

The response history of nonclassically damped systems can be determind by the extended modal analysis procedure (Chapter 14) or by numerical solution of the coupled equations of motion (Chapter 16). However, these approaches are not convenient for our objective to understand the dynamics of base-isolated buildings. Although, strictly speaking, classical modal analysis is not applicable to nonclassically damped systems, it can provide approximate results that suffice for our limited objective. This is the approach adopted here to determine the peak response of base-isolated structures to ground motion characterized by a design spectrum.

The two-DOF system that defines the one-story building on an isolation system is analyzed by the methods presented earlier in this book. With $\mathbf{m}$, $\mathbf{k}$, and $\mathbf{c}$ appropriately defined, Eq. (9.4.4) gives the equations of motion for the system; the natural vibration periods and modes of the system are determined following Example 10.4, and the earthquake

response of the system is estimated by response spectrum analysis following Section 13.8. The results of this analysis are presented next for an example system.

21.2.3 Effects of Base Isolation

To understand the dynamics of base isolation, let us consider a specific system: $m_b = 2m/3$, $T_f = 0.4$ sec, $T_b = 2.0$ sec, $\zeta_f = 2\%$, and $\zeta_b = 10\%$. The base shear V_b in the building and the base displacement u_b are to be estimated using the elastic design spectrum of Fig. 21.1.1, shown for damping ratios 2, 5, and 10%. For 5% damping this design spectrum is the same as in Fig. 6.9.5 scaled to peak ground acceleration of 0.5g. The other two spectra were constructed similarly using appropriate amplification factors from Table 6.9.1; these were shown earlier in Figs 6.9.9 and 6.9.10.

Observe that we have chosen damping in the structure as 2% of critical damping, lower than the 5% typically assumed in earthquake analysis and design of structures. As mentioned in Chapter 11, the higher damping value accounts for the additional energy dissipation through nonstructural damage expected in conventional structures at the larger motion during earthquakes. The aim of base isolation is to reduce the forces imparted to the structure to such a level that no damage to the structure or nonstructural elements occur and thus a lower value of damping is appropriate.

Vibration properties. The natural vibration periods T_n and modes ϕ_n of the one-story building on an isolation system are shown in Fig. 21.2.2. In the first mode the isolator undergoes deformation but the structure behaves as essentially rigid; this mode is therefore called the *isolation mode*. The natural period of this mode, $T_1 = 2.024$ sec, indicates that the isolation system period, $T_b = 2.0$ sec, is changed only slightly by flexibility of the structure. The second mode involves deformation of the structure as well as in the isolation system, and the structural deformation is larger. Therefore, this is called the *structural mode*, although as we shall see later, this mode contributes little to the earthquake-induced forces in the structure. The natural period of this mode, $T_2 = 0.25$ sec, is significantly shorter than the fixed-base period, $T_f = 0.4$ sec, of the structure. The natural periods of the combined system are more separate than the isolation system period T_b and fixed-base period T_f of the structure.

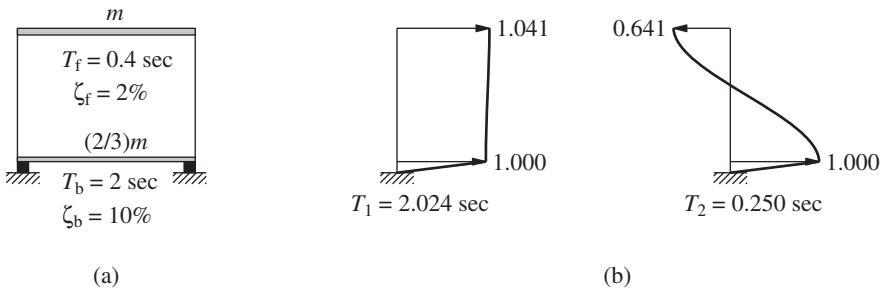

Figure 21.2.2 (a) One-story building on isolation system; (b) natural vibration modes and periods.

Modal static responses. Introduced in Section 13.2.1, the modal expansion of the effective earthquake force distribution, $\mathbf{s} = \mathbf{m1}$, for the system of Fig. 21.2.2a is shown in Fig. 21.2.3. These striking results indicate that the first-mode forces $\mathbf{s}_1$ are essentially the same as the total forces $\mathbf{s}$, and the second-mode forces $\mathbf{s}_2$ are very small. Static analysis of the system for forces $\mathbf{s}_n$ gives the modal static responses r_n^{st} for response quantity $r(t)$; see Table 13.2.1. In particular, for the base shear $V_b(t)$ in the structure and displacement $u_b(t)$ at the base, which is also the deformation of the isolation system, the modal static responses in the two modes are (see Fig. 21.2.3)

$$V_{b1}^{\text{st}} = 1.015m \qquad V_{b2}^{\text{st}} = -0.015m \tag{21.2.3a}$$

$$\omega_1^2 u_{b1}^{\text{st}} = 0.976 \qquad \omega_2^2 u_{b2}^{\text{st}} = 0.024 \tag{21.2.3b}$$

It is clear that the modal static responses for the second mode are negligible compared to the first mode. The second mode is therefore expected to contribute little to the earthquake response of the structure.

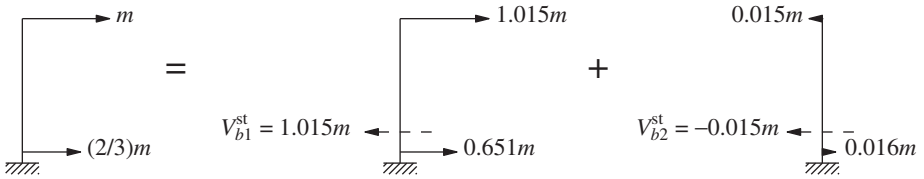

Figure 21.2.3 Modal expansion of effective earthquake forces and modal static responses for base shear.

Modal damping ratios. The modal damping ratios are determined by Eq. (10.9.11), repeated here for convenience:

$$\zeta_n = \frac{C_n}{2M_n\omega_n} \tag{21.2.4a}$$

where

$$M_n = \boldsymbol{\phi}_n^T \mathbf{m} \boldsymbol{\phi}_n \quad \text{and} \quad C_n = \boldsymbol{\phi}_n^T \mathbf{c} \boldsymbol{\phi}_n \tag{21.2.4b}$$

For the system chosen, these equations give

$$\zeta_1 = 9.65\% \qquad \zeta_2 = 5.06\% \tag{21.2.5}$$

Observe that the 9.65% damping in the first mode, the isolation mode, is very similar to the isolation-system damping, $\zeta_b = 10\%$; damping in the structure has little influence on modal damping in the isolation mode because the structure behaves as a rigid body for this mode. In contrast, high damping of the isolation system has increased the damping in the structural mode from 2% to 5.06%. Because damping in the system is nonclassical, the coupling terms $C_{21} = C_{12} = \boldsymbol{\phi}_1^T \mathbf{c} \boldsymbol{\phi}_2$ are nonzero and the modal equations are coupled (see Section 12.4). It is this coupling we are neglecting in using classical modal analysis for this system.

Peak modal and total responses. The peak value of the nth-mode contribution $r_n(t)$ to response $r(t)$ is given by Eq. (13.7.1), repeated here for convenience:

$$r_n = r_n^{\text{st}} A_n$$

where $A_n \equiv A(T_n, \zeta_n)$ is the ordinate of the pseudo-acceleration response (or design) spectrum at period T_n for damping ratio ζ_n. Specializing this equation for the two response quantities of interest, base shear V_b in the structure and isolator deformation u_b, gives

$$V_{bn} = V_{bn}^{\text{st}} A_n \qquad u_{bn} = (\omega_n^2 u_{bn}^{\text{st}}) D_n \tag{21.2.6}$$

where $D_n = A_n/\omega_n^2$ is the deformation spectrum ordinate. These calculations are summarized in Table 21.2.1 using the A_n values noted in Fig. 21.2.4; these were obtained for the actual damping values, Eq. (21.2.5), by using Table 6.9.2 instead of interpolating between the spectrum curves for 2, 5, and 10% damping. Observe that the response due to the second mode, the structural mode, is negligible although the pseudo-acceleration is large—because the modal static response is small. Obtained by combining modal responses by the SRSS combination rule, the deformation in the isolator is 14.042 in. and the base shear is 36.5% of the building weight excluding the base slab.

TABLE 21.2.1 CALCULATION OF BASE SHEAR AND ISOLATOR DEFORMATION

	Base Shear			Isolator Deformation		
Mode	A_n/g	V_{bn}^{st}/m	V_{bn}/w	D_n (in.)	$\omega_n^2 u_{bn}^{\text{st}}$	u_{bn} (in.)
1	0.359	1.015	0.365	14.390	0.976	14.042
2	1.347	−0.015	−0.021	0.823	0.024	0.020
SRSS			0.365			14.042

Reduction in base shear. The base shear is much larger if the structure is not isolated. This fixed-base structure has a natural vibration period $T_f = 0.4$ sec and damping ratio $\zeta_f = 2\%$. For these parameters the design spectrum of Fig. 21.2.4 gives $A(T_f, \zeta_f) = 1.830\text{g}$. Thus the base shear in the fixed-base structure is

$$V_b = mA(T_f, \zeta_f) = m(1.830\text{g}) \quad \text{or} \quad \frac{V_b}{w} = 1.830 \tag{21.2.7}$$

that is, 183% of the weight w of the building excluding the base slab, about five times the base shear in the isolated building.

The isolation system reduces the base shear primarily because the natural period of the first mode, the isolation mode, providing most of the response, is much longer than the fixed-base period of the structure, leading to a smaller spectral ordinate, as seen in Fig. 21.2.4. This becomes clear by reexamining the terms entering into the base shear due to the first mode:

$$V_{b1} = V_{b1}^{\text{st}} A_1 = (1.015m)(0.359\text{g}) \tag{21.2.8}$$

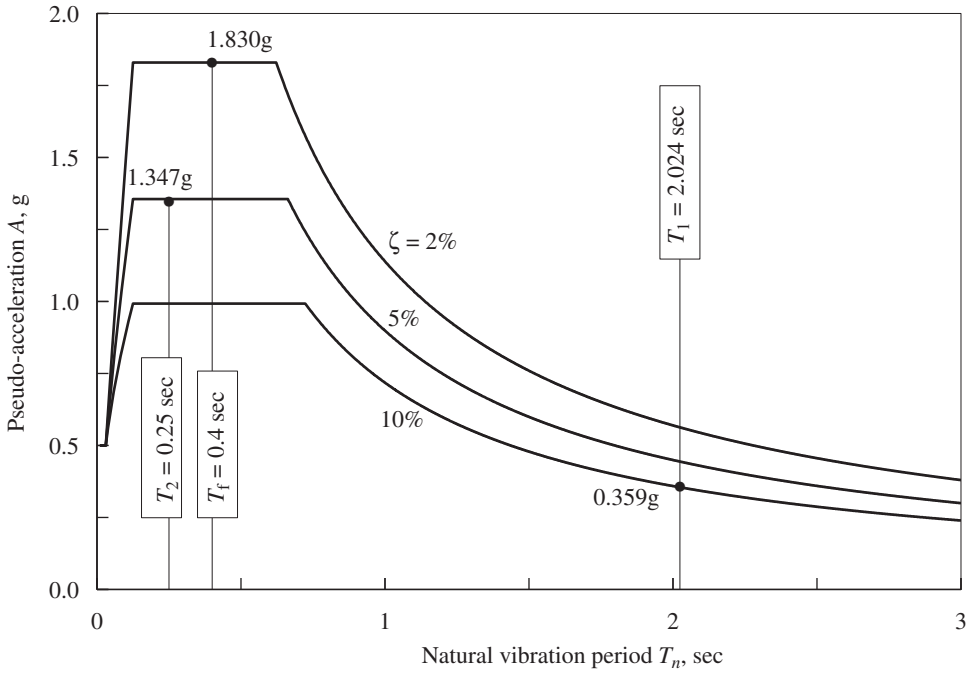

Figure 21.2.4 Design spectrum and spectral ordinates for fixed-base and isolated buildings.

Comparing Eq. (21.2.8) with (21.2.7a), it is apparent that because of the isolation system, the pseudo-acceleration is reduced from 1.830g to 0.359g, whereas the effective modal mass is essentially the same as the mass of the fixed-base building.

Why is base isolation effective? Base isolation lengthens the fundamental vibration period of the structure, and thus reduces the pseudo-acceleration for this mode (for the design spectrum considered) and hence the earthquake-induced forces in the structure. The second mode that produces deformation in the structure is essentially not excited by the ground motion, although its pseudo-acceleration is large. This can be explained as follows: The first vibration mode of the base-isolated structure involves deformation only in the isolation system, the structure above being essentially rigid. Thus the first-mode component $\mathbf{s}_1$ of the effective earthquake force distribution $\mathbf{s} = \mathbf{m1}$ is essentially the same as $\mathbf{s}$, and the second-mode component $\mathbf{s}_2$ is very small, causing very small modal static response in the second mode.

The primary reason for effectiveness of base isolation in reducing earthquake-induced forces in a building is the above-mentioned lengthening of the first-mode period. The damping in the isolation system and associated energy dissipation is only a secondary factor in reducing structural response.

21.2.4 Rigid-Structure Approximation

The base shear in the building and the deformation of the isolation system can be estimated by a simpler analysis treating the building as rigid. With this assumption the combined system has only one DOF. For this SDF system with natural period T_b and damping ratio ζ_b, the design spectrum gives the pseudo-acceleration $A(T_b, \zeta_b)$ and deformation $D(T_b, \zeta_b)$. Thus the isolator deformation is

$$u_b = D(T_b, \zeta_b) \tag{21.2.9}$$

and the base shear in the structure is

$$V_b = mA(T_b, \zeta_b) \tag{21.2.10}$$

The approximate results of Eqs. (21.2.9) and (21.2.10) are accurate for base-isolated systems if the period T_b of the isolation system (assuming rigid structure) is much longer than the fixed-base period T_f of the structure. This is illustrated using the system of Fig. 21.2.2: For $T_b = 2$ sec and $\zeta_b = 10\%$, the design spectrum gives $A(T_b, \zeta_b) = 0.359$g and $D(T_b, \zeta_b) = 14.036$ in., and Eq. (21.2.10) gives

$$V_b = m(0.359\text{g}) \quad \text{or} \quad \frac{V_b}{w} = 0.359 \tag{21.2.11}$$

Comparing Eq. (21.2.11) with Eq. (21.2.8), it is clear why this approximate analysis assuming a rigid structure gives almost "exact" results. Because the vibration properties with the rigid-structure assumption, $T_b = 2$ sec and $\zeta_b = 10\%$, are very close to the first-mode values, $T_1 = 2.024$ sec and $\zeta_1 = 9.65\%$, the spectral accelerations $A(T_b, \zeta_b)$ and $A(T_1, \zeta_1)$ are identical to three digits. Furthermore, the effective masses that enter into Eqs. (21.2.8) and (21.2.11) are essentially identical. Similarly, the isolator deformation from Eq. (21.2.9),

$$u_b = 14.036 \text{ in.} \tag{21.2.12}$$

is essentially identical to the first-mode response in Table 21.2.1.

Because of its accuracy, the rigid-structure approximation provides an expedient means to estimate the effectiveness of a base isolation system and to estimate the isolator deformation. First, the ratio $A(T_b, \zeta_b)/A(T_f, \zeta_f)$ of two spectral ordinates gives the base shear in the isolated system as a fraction of the base shear in the fixed-base structure. Second, the deformation spectrum ordinate $D(T_b, \zeta_b)$ is the isolator deformation.

21.3 EFFECTIVENESS OF BASE ISOLATION

It is clear that the effectiveness of base isolation in reducing structural forces is closely tied to the lengthening of the natural period of the structure, and for this purpose the period ratio T_b/T_f should be as large as practical. In the example of the preceding section, the natural period of the fixed-base structure located the structure at the peak of the selected design spectrum. With base isolation, the natural period (of the isolation mode contributing almost all of the response) was shifted to the velocity-sensitive region of the spectrum with much smaller pseudo-acceleration. As a result, the base shear is reduced from 183% of the

structural weight (excluding the base slab) to 36.5%. Whether the forces in the structure are reduced because of this period shift depends on the natural period of the fixed-base structure and on the shape of the earthquake design spectrum, among other factors. We illustrate these concepts next.

First, consider the same one-story building and base isolation system as in the preceding section to be located in Mexico City at the site where ground motions recorded during the 1985 earthquake produced the response spectrum shown in Fig. 21.3.1. Noted on this spectrum are the pseudo-acceleration values $A(T_f, \zeta_f) = 0.25\text{g}$ corresponding to $T_f = 0.4$ sec and $\zeta_f = 2\%$ for the fixed-base structure and $A(T_b, \zeta_b) = 0.63\text{g}$ associated with $T_b = 2.0$ sec and $\zeta_b = 10\%$ for the isolated structure (with the building assumed to be rigid). The ratio $A(T_b, \zeta_b)/A(T_f, \zeta_f) = 0.63\text{g}/0.25\text{g} = 2.52$ implies that the base shear in the isolated structure is approximately 2.52 times the base shear in the fixed-base structure. In this case base isolation is not helpful; in fact, it is harmful.

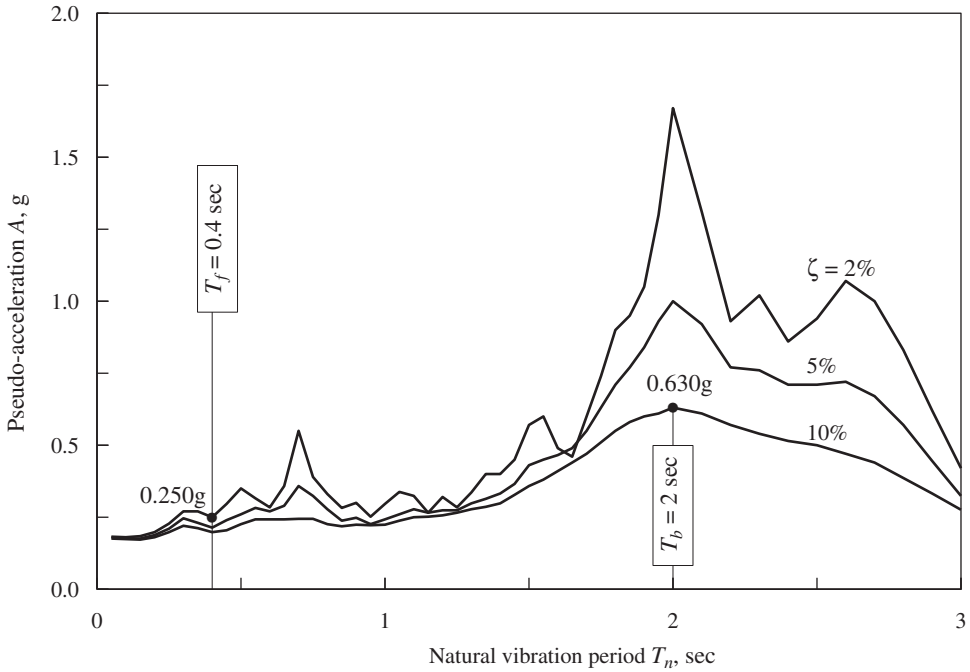

Figure 21.3.1 Response spectrum for ground motion recorded on September 19, 1985, at SCT site in Mexico City and spectral ordinates for fixed-base and isolated buildings.

Next, consider a structure with a relatively long fixed-base period and the ground motion characterized by the original design spectrum (Fig. 21.1.1). In this case we shall see that base isolation is only slightly beneficial—much less than when the fixed-base period was relatively short. To illustrate these results, consider a structure with a fixed-base period of 2 sec with other parameters for the structure and isolation system as before. Thus the system parameters are $T_f = 2$ sec, $\zeta_f = 2\%$, $m_b = \frac{2}{3}m$, $T_b = 2$ sec, and $\zeta_b = 10\%$.

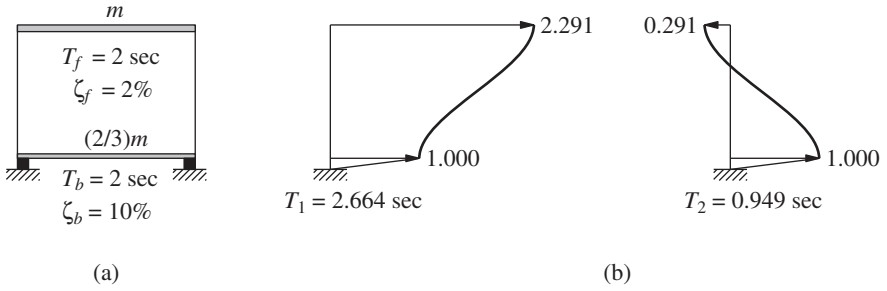

Figure 21.3.2 (a) One-story building on isolation system; (b) natural vibration modes and periods.

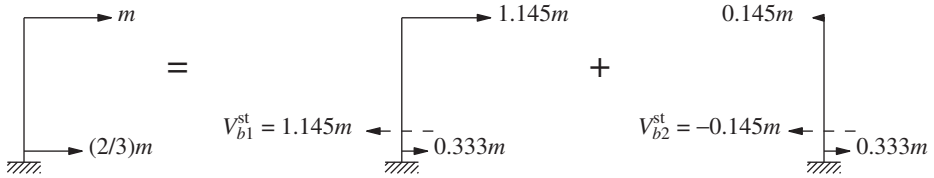

Figure 21.3.3 Modal expansion of effective earthquake forces and modal static responses for base shear.

Analysis of this system with $T_b = T_f$ by the procedures used for the example of Section 21.2 gives the natural vibration periods and modes (Fig. 21.3.2), the modal expansion of the effective earthquake force distribution: $\mathbf{s} = \mathbf{m1}$ (Fig. 21.3.3), and the modal damping ratios: 4.50% and 12.64%. In contrast to the previous system with $T_b >> T_f$: (1) the structure does not behave as rigidly in the first mode, and this natural period is significantly affected by the flexibility of the structure; (2) the second-mode contribution to the effective earthquake forces is no longer negligible; and (3) the first-mode damping of 4.5% is no longer close to the isolation system damping of 10%.

A summary of the calculations to obtain the base shear and isolator deformation is presented in Table 21.3.1, with the spectral values identified in Fig. 21.3.4. In contrast

TABLE 21.3.1 CALCULATION OF BASE SHEAR AND ISOLATOR DEFORMATION

	Base Shear			Isolator Deformation		
Mode	A_n/g	V_{bn}^{st}/m	V_{bn}/w	D_n (in.)	$\omega_n^2 u_{bn}^{st}$	u_{bn} (in.)
1	0.348	1.145	0.398	24.136	0.500	12.068
2	0.691	−0.145	−0.101	6.095	0.500	3.047
SRSS			0.411			12.447

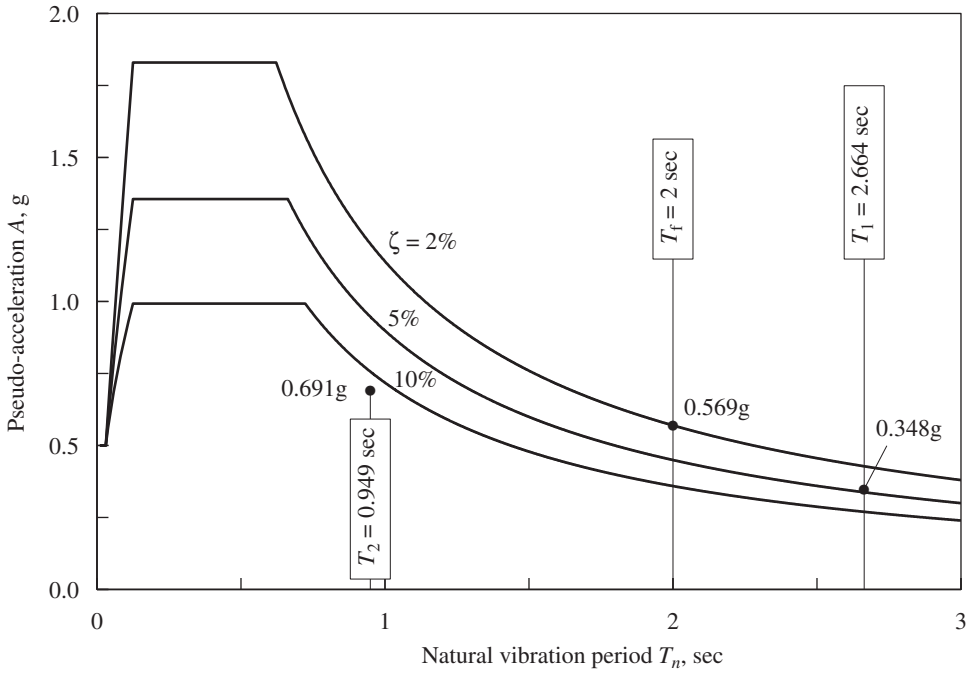

Figure 21.3.4 Design spectrum and spectral ordinates for fixed-base and isolated buildings.

to the previous system with $T_b >> T_f$, the response of the second mode is significant, although it does not contribute much when it is combined—using the SRSS rule—with the first-mode response. We find the isolator deformation to be 12.447 in., and the base shear is 41.1% of the structural weight, excluding that of the base slab.

The fixed-base structure has a natural period $T_f = 2$ sec and damping ratio $\zeta_f = 2\%$, and the corresponding spectral ordinate is $A(T_f, \zeta_f) = 0.569$g (Fig. 21.3.4). Thus if the structure were not isolated, the base shear is

$$V_b = mA(T_f, \zeta_f) \quad \text{or} \quad \frac{V_b}{w} = 0.569 \tag{21.3.1}$$

(i.e., 56.9% of the building weight). It is clear that some benefit is obtained by base isolation, although it is much less than if the vibration period of the structure had been shorter, as in the original example. It is for this reason that base isolation is rarely used for structures with natural period well into the velocity-sensitive region of the spectrum.

In passing we also note that the approximate analysis based on the assumption of a rigid structure is not accurate for a structure with a relatively long natural period. The approximate analysis gives a base shear coefficient of 35.9%, Eq. (21.2.11), compared to 41.1% from the complete analysis. The isolator deformation from the approximate analysis is 14.036 in., Eq. (21.2.12), compared to 12.447 in. from the complete analysis.

21.4 BASE-ISOLATED MULTISTORY BUILDINGS

In the preceding sections we were able to identify the underlying reasons for the effectiveness of a base isolation system by studying the dynamics of a one-story building. In this section we investigate how the dynamics of a multistory building is modified by base isolation. As before, we assume the system to be linear. We will see that the key concepts underlying base isolation, identified by the dynamics of one-story systems, carry over to multistory systems.

21.4.1 System Considered and Parameters

The N-story building to be isolated is shown idealized in Fig. 21.4.1a. On a fixed base, this system is defined by mass matrix $\mathbf{m}_f$, damping matrix $\mathbf{c}_f$, and stiffness matrix $\mathbf{k}_f$, which can be constructed by the methods developed in Chapters 9 and 11; the subscript f denotes "fixed base." If the mass of the structure is idealized as lumped at the floor levels, as shown in Fig. 21.4.1a, $\mathbf{m}_f$ is a diagonal matrix with diagonal element $m_{jj} = m_j$, the mass lumped at the jth floor. The total mass of the building, $M = \sum m_j$. The natural periods and modes of vibration of the fixed-base system are denoted by T_{nf} and ϕ_{nf}, respectively, where $n = 1, 2, \ldots, N$. Damping in the structure is assumed to be of classical form and defined by modal damping ratios ζ_{nf}, $n = 1, 2, \ldots, N$.

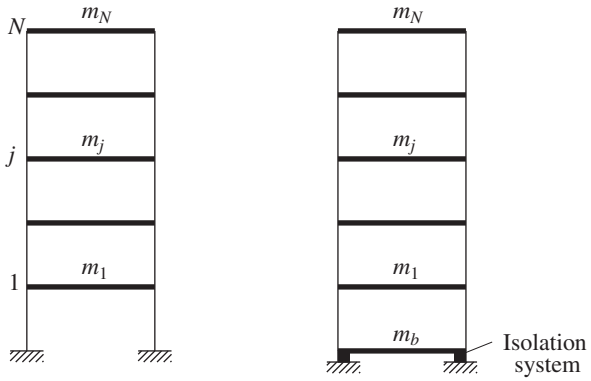

Figure 21.4.1 (a) Fixed-base N-story building; (b) isolated N-story building.

As shown in Fig. 21.4.1b, this N-story building is mounted on a base slab of mass m_b, supported in turn on a base isolation system with lateral stiffness k_b and linear viscous damping c_b. As in Section 21.2, two parameters, T_b and ζ_b, are introduced to characterize the isolation system:

$$T_b = \frac{2\pi}{\omega_b} \qquad \text{where} \quad \omega_b = \sqrt{\frac{k_b}{M + m_b}} \tag{21.4.1a}$$

$$\zeta_b = \frac{c_b}{2(M + m_b)\omega_b} \tag{21.4.1b}$$

As before, we may interpret T_b as the natural vibration period and ζ_b the damping ratio of the isolation system (with the building assumed to be rigid). For base isolation to be effective in reducing the earthquake-induced forces in the building, T_b must be much longer than T_{1f}, the fundamental period of the fixed-base building.

The N-story building on a base isolation system is an $(N + 1)$-DOF system with nonclassical damping because damping in the isolation system is typically much more than in the building. The mass, stiffness, and damping matrices of order $N + 1$ for the combined system are denoted by $\mathbf{m}$, $\mathbf{k}$, and $\mathbf{c}$, respectively.

21.4.2 Analysis Procedure

With ground motion characterized by a design spectrum, the RSA procedure of Chapter 13, Part B, will be used to analyze two systems: (1) a building on a fixed base, and (2) the same structure supported on an isolation system. In applying the RSA procedure to the isolated structure we are ignoring the coupling of modal equations due to nonclassical damping, typical of structures on isolation systems. The modal damping ratios of the isolated structure are given by Eq. (21.2.4). We focus on two response quantities: base shear in the building and the base displacement (or isolator deformation). The peak responses due to the nth mode of vibration are determined using Eq. (21.2.6), and these peak modal responses are combined by the SRSS rule. The results of such analyses are presented next for an example system.

21.4.3 Effects of Base Isolation

To understand how base isolation affects the dynamics of buildings, we consider a specific system. The fixed-base structure is a five-story shear frame (i.e., beam-to-column stiffness ratio $\rho = \infty$) with mass and stiffness properties uniform over its height: lumped mass $m = 100$ kips/g at each floor, and stiffnesses k for each story; k is chosen so that the fundamental natural vibration period $T_{1f} = 0.4$ sec. The classical damping matrix $\mathbf{c}_f = a_1\mathbf{k}_f$ with a_1 chosen to obtain 2% damping in the fundamental mode. The base slab mass $m_b = m$ and the stiffness and damping of the isolation system are such that $T_b = 2.0$ sec and $\zeta_b = 10\%$ [Eq. (21.4.1)]. In this section we examine the vibration properties—natural periods and natural modes—modal damping ratios, and the earthquake response of two systems: (1) this five-story building on a fixed base, and (2) the same five-story building supported on the isolation system described above. The earthquake excitation is characterized by the design spectrum of Fig. 21.1.1.

Vibration properties. The natural vibration periods and modes of both systems are presented in Fig. 21.4.2 and Table 21.4.1. The fixed-base structure has the familiar mode shapes and ratios of natural periods. In the first mode of the isolated building, the isolator undergoes deformation but the building behaves as essentially rigid; this mode is therefore called the isolation mode. The natural period of this mode, $T_1 = 2.030$ sec, indicates that the isolation-system period, $T_b = 2.0$ sec, is changed only slightly by the flexibility of the structure. The other modes involve deformation in the structure as well as in the isolation system. We refer to these modes as structural modes, although as we shall

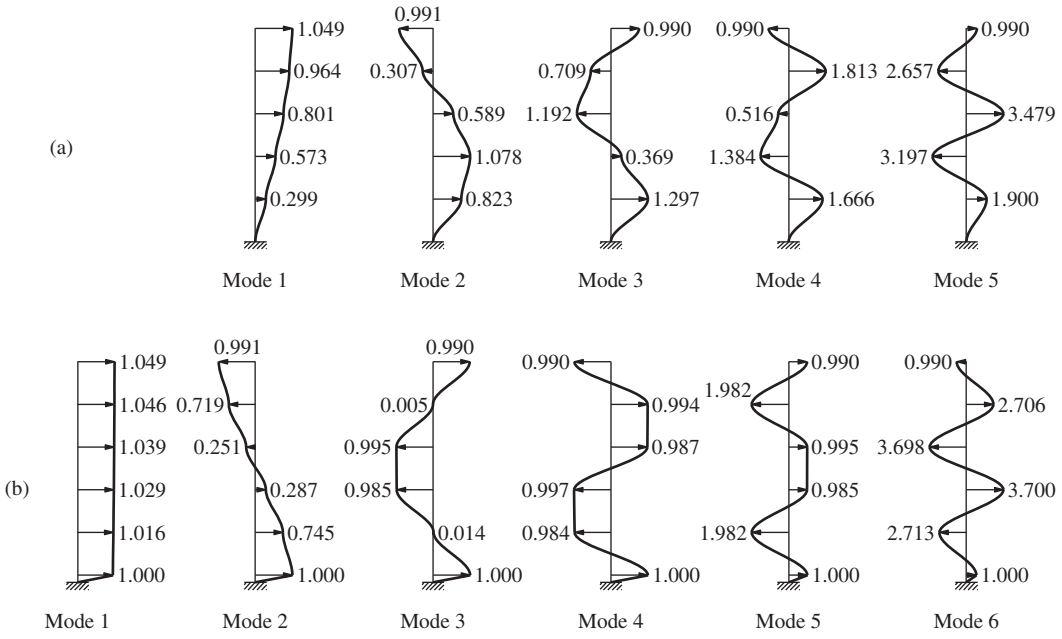

Figure 21.4.2 Natural vibration modes: (a) fixed-base building; (b) isolated building.

TABLE 21.4.1 NATURAL PERIODS AND MODAL DAMPING RATIOS

Fixed-Base Building			Isolated Building		
Mode	T_{nf} (sec)	ζ_{nf} (%)	Mode	T_n (sec)	ζ_n (%)
			1	2.030	9.58
1	0.400	2.00	2	0.217	5.64
2	0.137	5.84	3	0.114	7.87
3	0.087	9.20	4	0.080	10.3
4	0.068	11.8	5	0.066	12.3
5	0.059	13.5	6	0.059	13.6

see later, these modes contribute little to the earthquake-induced forces in the structure. It is clear that the isolation system has a large effect on the natural period of the first structural mode but a decreasing effect on the higher-mode periods. In these higher modes the motion of the base mass decreases relative to the structural motions, and the base mass is acting essentially as a fixed base.

Modal damping ratios. The modal damping ratios for both systems are presented in Table 21.4.1. The modal damping ratios for the fixed-base structure decrease linearly with natural period (i.e., increase linearly with natural frequency) because the damping is stiffness proportional (Section 11.4.1). The damping of 9.58% in the first mode

of the isolated building, the isolation mode, is very similar to the isolation-system damping, $\zeta_b = 10\%$; damping in the structure has little influence on modal damping because the structure remains essentially rigid in this mode. The high damping of the isolation system has increased the damping in the first structural mode from 2.0% to 5.64%, but to a smaller degree in the higher modes.

Modal static responses. We now compare the modal static response in the natural modes of both systems, the fixed-base and isolated buildings. The modal components $\mathbf{s}_n$ of the effective earthquake force distribution, $\mathbf{s} = \mathbf{m1}$, are shown in Fig. 13.2.4 for the fixed-base structure and in Fig. 21.4.3 for the base-isolated structure.† In the latter case, forces in the first mode, the isolation mode, are essentially the same as the total forces, and the forces associated with all the structural modes are very small. Static analysis of both systems for their respective modal forces gives the modal static shears V_{bn}^{st} at the base of the structure and modal static base displacements or isolator deformations u_{bn}^{st}; see Table 13.2.1. The results are given in Tables 21.4.2 and 21.4.3. It is clear that V_{bn}^{st} has

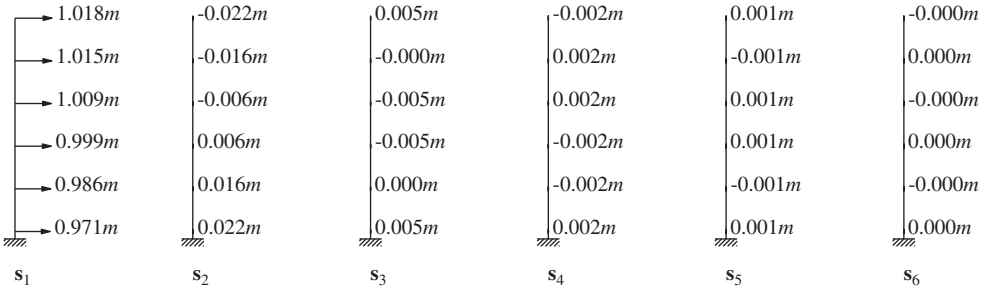

Figure 21.4.3 Modal components of effective earthquake forces for a five-story building on isolation system.

TABLE 21.4.2 CALCULATION OF BASE SHEAR IN FIXED-BASE AND ISOLATED BUILDINGS

Fixed-Base Building				Isolated Building			
Mode	A_n/g	V_{bn}^{st}/m	V_b/W	Mode	A_n/g	V_{bn}^{st}/m	V_b/W
				1	0.359	5.028	0.361
1	1.830	4.398	1.609	2	1.291	−0.021	−0.005
2	1.272	0.436	0.111	3	1.058	−0.005	−0.001
3	0.859	0.121	0.021	4	0.792	−0.002	−0.000
4	0.700	0.038	0.005	5	0.682	−0.0005	−0.000
5	0.638	0.008	0.001	6	0.635	−0.0001	−0.000
SRSS			1.613	SRSS			0.361

†Figure 13.2.4 is valid for this uniform five-story shear frame because its vibration modes are the same as those of the system considered in Section 13.2.6, although the story stiffness (and natural vibration periods) of the two systems are different.

TABLE 21.4.3 CALCULATION OF ISOLATOR DEFORMATION

Mode	D_n	$\omega_n^2 u_{bn}^{st}$	u_{bn} (in.)
1	14.470	0.971	14.045
2	0.597	0.022	0.013
3	0.133	0.005	0.001
4	0.050	0.002	0.000
5	0.029	0.001	0.000
6	0.022	0.0001	0.000
SRSS			14.045

significant values in the first two modes of the fixed-base structure. However, for the isolated building, V_{bn}^{st} is small in all the structural modes, and the response in these modes is expected to be negligible. The isolation mode provides the dominant value V_{b1}^{st} and therefore will provide most of the response.

Peak modal and total responses. The peak value of the earthquake response due to each natural mode of both systems is determined from Eq. (21.2.6), where the spectral ordinates A_n/g are shown in Figs. 21.4.4 and 21.4.5 and $D_n = A_n/\omega_n^2$. These peak

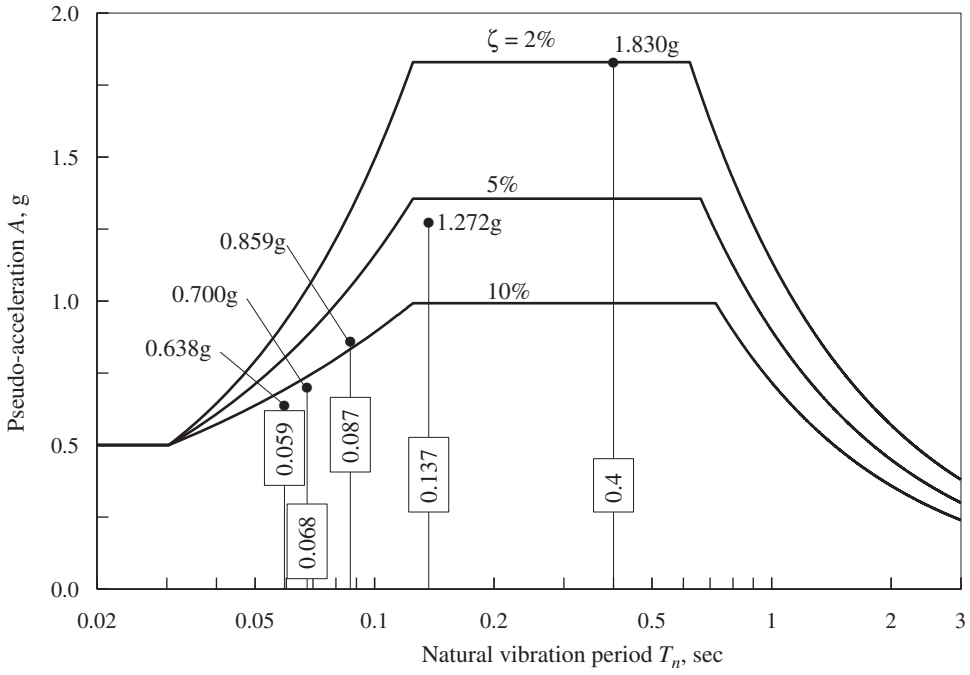

Figure 21.4.4 Design spectrum and spectral ordinates for fixed-base five-story building.

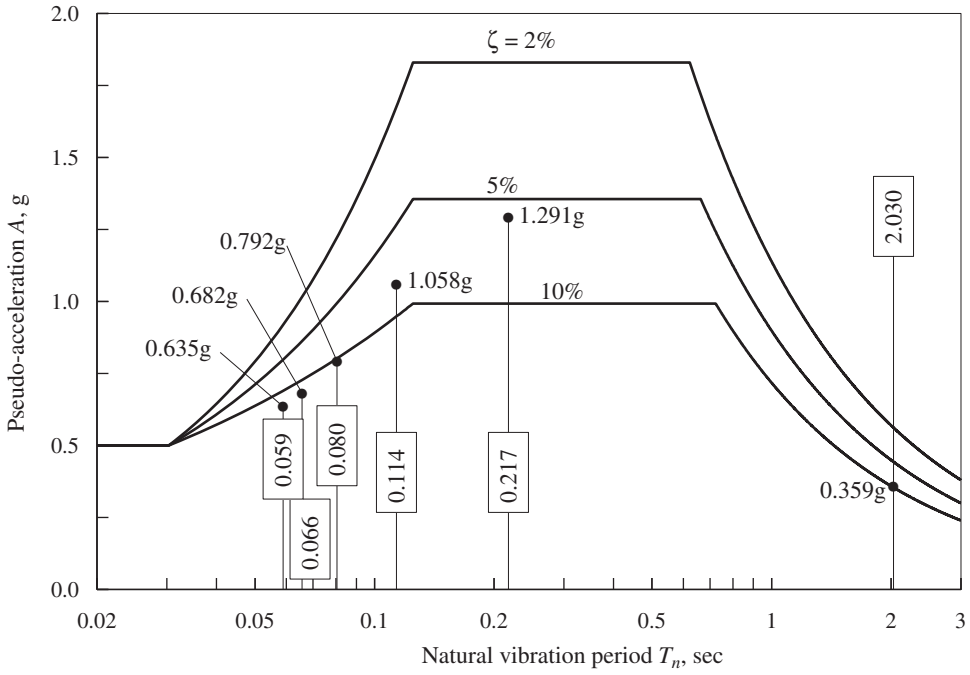

Figure 21.4.5 Design spectrum and spectral ordinates for five-story building on isolation system.

modal responses are presented in Tables 21.4.2 and 21.4.3 together with their combined value determined by the SRSS rule. Observe that as predicted from the modal static responses, the dynamic response of the isolated building due to all its structural modes is negligible although their pseudo-accelerations are large. The isolation mode alone produces essentially the entire response: isolation system deformation of 14.045 in. and base shear equal to 36.1% of W, the 500-kip weight of the building excluding that of the base slab. The response in the first two modes of the fixed-base building is significant; however, the second mode contributes little to the SRSS-combined value of 161.3% of W.

Reduction in base shear. To understand the underlying reasons for this drastic reduction in base shear, we examine the peak modal responses in both fixed-base and isolated systems. Each peak modal response is the product of two parts: the modal static response V_{bn}^{st} and the pseudo-acceleration A_n. Each part is examined for the first mode of the base-isolated building and of the fixed-base building; this is the mode that provides most of the response in each case. Observe that $V_{b1}^{\text{st}} = 5.028m$ for the isolated building, which is slightly larger than $V_{b1}^{\text{st}} = 4.398m$ for the fixed-base building. However, $A_1 = 0.359\text{g}$ for the isolated building (Fig. 21.4.5) is only one-fifth of $A_1 = 1.830\text{g}$ for the fixed-base building (Fig. 21.4.4); as a result, the first-mode base shear coefficient of 36.1% in the base-isolated building is much smaller than 160.9% for the fixed-base building.

Why is base isolation effective? The isolation system reduces the base shear primarily because the natural vibration period of the isolation mode, providing most of the response, is much longer than the fundamental period of the fixed-base structure, leading to a much smaller spectral ordinate. This is typical of design spectra on firm ground and fixed-base structures with fundamental period in the flat portion of the acceleration-sensitive region of the spectrum. The higher modes are essentially not excited by the ground motion—although their pseudo-accelerations are large—because their modal static responses are very small.

The primary reason for effectiveness of base isolation in reducing earthquake-induced forces in a building is the above-mentioned lengthening of the first mode period. The damping in the isolation system and associated energy dissipation is only a secondary factor in reducing structural response.

21.4.4 Rigid-Structure Approximation

The base shear in the isolated building and the deformation of the isolation system can be estimated by a simpler analysis, treating the building as rigid. The natural period of the resulting SDF system is T_b and its damping ratio is ζ_b [Eq. (21.4.1)]; the associated design spectrum ordinates are $A(T_b, \zeta_b)$ for the pseudo-acceleration and $D(T_b, \zeta_b)$ for the deformation. Thus the base shear in the structure and the isolator deformation are

$$V_b = MA(T_b, \zeta_b) \qquad u_b = D(T_b, \zeta_b) \tag{21.4.2}$$

This approximate procedure will provide excellent results if the isolation-system period T_b is much longer than the fundamental period T_{1f} of the fixed-base structure. This is illustrated using the system of Fig. 21.4.1b, analyzed earlier. For this system, $T_b = 2.0$ sec and $\zeta_b = 10\%$ and the spectral values are $A(T_b, \zeta_b) = 0.359$g and $D(T_b, \zeta_b) = 14.036$ in., as noted in Section 21.2.4. Substituting these values in Eq. (21.4.2) gives

$$V_b = 0.359W \qquad u_b = 14.036 \text{ in.} \tag{21.4.3}$$

which are essentially identical to the responses due to the isolation mode (and to the total response) presented in Tables 21.4.2 and 21.4.3.

21.5 APPLICATIONS OF BASE ISOLATION

Base isolation provides an alternative to the conventional, fixed-base design of structures and may be cost-effective for some new buildings in locations where very strong ground shaking is likely. It is an attractive alternative for buildings that must remain functional after a major earthquake (e.g., hospitals, emergency communications centers, computer processing centers). Several new buildings have been isolated using rubber (or elastomeric) bearings or FPS isolators; these examples are described in references at the end of this chapter.

Figure 21.5.1 San Francisco City Hall. (Courtesy of S. Nasseh.)

Both types of isolation systems have also been used for retrofit of existing buildings that are brittle and weak: for example, unreinforced masonry buildings or reinforced-concrete buildings of early design, not including the type of detailing of the reinforcement necessary for ductile performance. Conventional seismic strengthening designs require adding new structural members, such as shear walls, frames, and bracing. Base isolation minimizes the need for such strengthening measures by reducing the earthquake forces imparted to the building. It is therefore an attractive retrofit approach for buildings of historical or architectural merit whose appearance and character must be preserved. Many examples of retrofitting existing buildings are described in end-of-chapter references. However, it is difficult and expensive to construct a new foundation system for the isolators, to modify the base of the building so that it can be supported on isolators, and to shore up the building during construction of the isolation and foundation systems.

A good example of a retrofit application of laminated-rubber-bearing-isolation systems is the San Francisco City Hall in San Francisco, California. Constructed in 1915 to replace the previous structure that was destroyed in the 1906 San Francisco earthquake, this building is an outstanding example of classical architecture and is listed in the National Register of Historic Places (Fig. 21.5.1). The five-story building with its dome rising 300 ft above the ground floor is 309 ft by 408 ft in plan, occupying two city blocks. The structural system is a steel frame and concrete slabs with unreinforced brick masonry integral with the granite cladding, hollow clay tile infill walls, and limestone or marble panels lining many of the interior spaces.

Substantial damage sustained from the 1989 Loma Prieta earthquake, centered about 60 miles away, necessitated repairs and strengthening. The fixed-base fundamental period of vibration of the building is approximately 0.9 sec, implying that large ductility demands can be imposed on the structure by strong shaking expected at the building site from an earthquake centered on a nearby segment of the San Andreas fault. To improve the earthquake resistance of this structure, base isolation was adopted especially because it preserved the historic fabric of this building. In addition, the superstructure was strengthened by new shear walls in the interior of the building. This retrofit project was completed in 1998.

The isolation system consisted of 530 isolators, each a laminated rubber bearing with lead plugs, located at the base of each column and at the base of the shear walls (Fig. 21.5.2). The 21-in.-high bearings varied from 31 to 36 in. in diameter. The columns are supported on one or more isolators under a cruciform-shaped steel structure; multiple isolators were provided for the heavily loaded columns. Installation of the isolators proved to be very complicated and required shoring up the columns, cutting the columns, and transferring the column loads to temporary supports. The plane of isolation is just above the existing foundation.

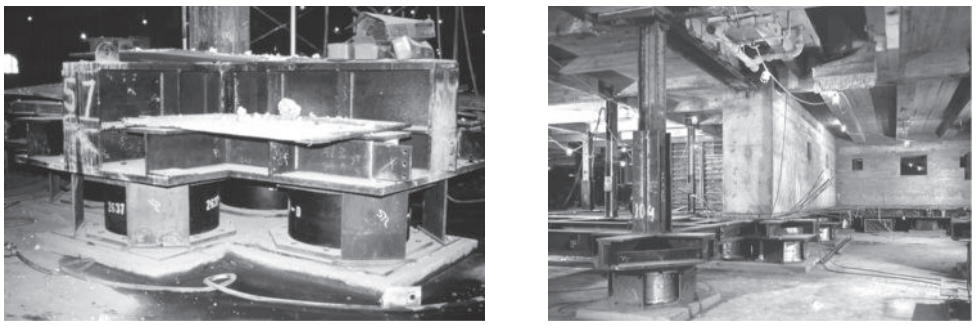

(a) (b)

Figure 21.5.2 San Francisco City Hall: laminated rubber bearings at the base of (a) columns and (b) shear walls. [(a) Courtesy of J. M. Kelly; (b) Robert Canfield photo, courtesy of S. Nasseh.]

The isolated building is estimated to move 18 to 26 in. at an isolation period of 2.5 sec for a design earthquake with peak ground acceleration of 0.4g. To permit this motion, a moat was constructed around the building to provide a minimum seismic gap of 28 in. Flexible joints were provided for utilities—plumbing, electrical, and telephone lines—crossing this moat space to accommodate movement across the isolation system.

A good example of new construction using base isolation is the new (completed in 2000) International Terminal at the San Francisco Airport (Figs. 21.5.3 and 21.5.4), which was designed to remain operational after a Magnitude 8 earthquake on the San Andreas Fault approximately 3 miles away. To achieve this performance goal it was

Figure 21.5.3 International Terminal at San Francisco Airport. (T. Hursley, photo, courtesy of Skidmore, Owings, & Merrill LLP.)

Figure 21.5.4 International Terminal at San Francisco Airport. (T. Hursley, photo, courtesy of Skidmore, Owings, & Merrill LLP.)

Figure 21.5.5 International Terminal at San Francisco Airport: FPS bearing at base of column. (P. Lee, photo, courtesy of Skidmore, Owings, & Merrill LLP.)

decided to isolate the superstructure, which consists of steel concentric and eccentric braced frames with fully welded moment connections.

The isolation system consists of 267 isolators, one at the base of each column (Fig. 21.5.5). Each isolator is a friction pendulum sliding bearing. The cast steel bearing consists of a stainless steel spherical surface and articulated slider, which allows a lateral displacement up to 20 in. and provides an isolation period of 3 sec.

Base isolation had the effect of reducing the earthquake force demands on the superstructure to 30% of the demands for a fixed-base structure. With this force reduction it was feasible to design the superstructure to remain essentially elastic and hence undamaged under the selected design earthquake with peak ground acceleration of 0.6g.

FURTHER READING

Kelly, J. M., *Earthquake Resistant Design with Rubber*, 2nd ed., Springer-Verlag, London, 1996, Chapters 1, 3, and 4.

Naeim, F., and Kelly, J. M., *Design of Seismic Isolated Structures: From Theory to Practice*, Wiley, Chichester, U.K., 1999.

Seismic Isolation: From Idea to Reality, theme issue of *Earthquake Spectra*, **6**, 1990, pp. 161–432.

Skinner, R. I., Robinson, W. H., and McVerry, G. H., *An Introduction to Seismic Isolation*, Wiley, Chichester, U.K., 1993.

Warburton, G. B., *Reduction of Vibrations*, The 3rd Mallet–Milne Lecture, Wiley, Chichester, U.K., 1992, pp. 21–46.

22

Structural Dynamics in Building Codes

PREVIEW

Most seismic building codes permit the use of a static equivalent lateral force (ELF) procedure for many regular structures with relatively short periods. For other structures, dynamic analysis procedures are required. According to the ELF procedure, structures are designed to resist specified *static* lateral forces related to the properties of the structure and the seismicity of the region. Based on an estimate of the fundamental natural vibration period of the structure, formulas are specified for the base shear and the distribution of lateral forces over the height of the building. Static analysis of the building for these forces provides the design forces, including shears and overturning moments for the various stories, with some codes permitting reductions in the statically computed overturning moments. These seismic design provisions in four building codes—*International Building Code* (United States),[†] *National Building Code of Canada, Mexico Federal District Code,* and *Eurocode 8*—are presented in Part A of this chapter together with their relationship to the theory of structural dynamics developed in Chapters 6, 7, 8, and 13. The code provisions presented are not complete; those provisions that we are unprepared to evaluate based on this book have been excluded or only mentioned: effects of local soil conditions, torsional moments about a vertical axis, combination of earthquake forces due to the simultaneous action of ground motion components, and the requirements for detailing structures to ensure ductile behavior, among others. In Part B of the chapter the code provisions are evaluated in light of the results of the dynamic analysis of buildings, discussed in Chapters 19 and 20.

[†]In the 2009 IBC, most of the technical requirements are adopted by reference to the ASCE 7-05 document.